IMMUNOBIOLOGY

LAMP1/CD107a is required for efficient perforin delivery to lytic granules and NK-cell cytotoxicity

Konrad Krzewski, Aleksandra Gil-Krzewska, Victoria Nguyen, Giovanna Peruzzi, and John E. Coligan

Receptor Cell Biology Section, Laboratory of Immunogenetics, National Institute of Allergy and Infectious Diseases, National Institutes of Health, Rockville, MD

Key Points

- LAMP1 silencing inhibits cytotoxicity of human NK cells.
- LAMP1 is important for perforin trafficking to the lytic granules and granule movement.

Secretory lysosomes of natural killer (NK) cells, containing perforin and granzymes, are indispensable for NK-cell cytotoxicity because their release results in the induction of target-cell apoptosis. Lysosome-associated membrane protein (LAMP) 1/CD107a is used as a marker for NK-cell degranulation, but its role in NK-cell biology is unknown. We show that LAMP1 silencing causes inhibition of NK-cell cytotoxicity, as LAMP1 RNA interference (RNAi) cells fail to deliver granzyme B to target cells. Reduction of LAMP1 expression affects the movement of lytic granules and results in decreased levels of perforin, but not granzyme B, in the granules. In LAMP1 RNAi cells, more perforin is retained outside of lysosomal compartments in *trans*-Golgi network–derived transport vesicles. Disruption of expression of LAMP1 binding partner, adaptor protein 1 (AP-1) sorting complex, also causes retention of perforin in the transport vesicles and inhibits cytotoxicity, indicating that the interaction between AP-1 sorting complex and LAMP1 on the surface of the transport vesicles is important for perforin trafficking to lytic granules. We conclude that the decreased level of perforin in lytic granules of LAMP1-deficient cells, combined with disturbed motility of the lytic granules, leads to the inability to deliver apoptosis-inducing granzyme B to target cells and to inhibition of NK-cell cytotoxicity. (*Blood*. 2013;121(23):4672-4683)

Introduction

Natural killer (NK) cells comprise a subset of lymphocytes involved in protection against microbial pathogens and tumors.[1] Because of their cytotoxic capacity, NK cells are able to directly eliminate abnormal cells. The killing of these target cells is a multistage process that culminates with the localized secretion of lytic granules, containing perforin and granzymes, at the immunologic synapse.[2,3] Upon delivery to a target cell, perforin generates pores in the membranes,[3-5] allowing granzymes to access target-cell cytoplasm and induce apoptosis.[3,6,7] Defects in lytic granule secretion are associated with serious diseases, such as hemophagocytic lymphohistiocytosis and Chediak-Higashi, Hermansky-Pudlak, or Griscelli syndrome.[8-11] Knowledge about the proteins involved in regulation of lytic granule release is very limited. Soluble *N*-ethylmaleimide-sensitive factor attachment protein receptor proteins and small guanosine triphosphatases have been shown to be required for NK-cell degranulation and tumor killing,[12-16] but the granule-specific protein machinery involved in NK-cell exocytosis is poorly understood.

Lytic granules have the characteristics of lysosomes and are referred to as "secretory lysosomes."[17,18] There are many proteins residing in lysosomal membranes that function in acidification of the lysosomal lumen, protein import, membrane fusion, and transport of degradation products to the cytoplasm.[19] Surprisingly, the role of the most abundant proteins, lysosome-associated membrane protein (LAMP) 1 and LAMP2 (CD107a and CD107b, respectively), is largely unknown. In humans, mutations in LAMP2 cause Danon disease, believed to arise from aberrant autophagy.[20] LAMP2-deficient mice also accumulate autophagic vacuoles in several tissues.[21] LAMP1-deficient mice have an almost normal phenotype but have elevated levels of LAMP2, suggesting that LAMP2 can compensate for the loss of LAMP1.[22] Recent studies using LAMP-depleted fibroblasts demonstrate that both proteins are required for proper lysosomal transport and efficient (auto)phagosome-lysosome fusion.[23,24]

Although LAMP1 is widely used as a marker for the identification of NK-cell degranulation,[25] as it appears on the cell surface following the fusion of lysosomes with the plasma membrane, the role of LAMP1 in NK-cell biology is unknown. Since LAMP1 is one of the most abundant proteins in the lysosomal membrane and NK cells use their lysosomes to induce the death of target cells, we sought to determine the importance of LAMP1 in NK-cell cytolytic activity.

Methods

Please refer to the supplemental Methods (see the *Blood* Web site) for the detailed description of methods and reagents used.

Antibodies

Antibodies (Ab's) used included the following: anti-LAMP1, anti-LAMP2, and anti–granzyme B (Santa Cruz Biotechnology or eBiosciences);

Submitted August 31, 2012; accepted April 22, 2013. Prepublished online as *Blood* First Edition paper, April 30, 2013; DOI 10.1182/blood-2012-08-453738.

The online version of this article contains a data supplement.

The publication costs of this article were defrayed in part by page charge payment. Therefore, and solely to indicate this fact, this article is hereby marked "advertisement" in accordance with 18 USC section 1734.

anti–Early Endosome Antigen 1 (EEA-1), anti-p150^{glued}, and anti–adaptin γ, α, and β (BD); anti–Ras-associated binding (Rab)7 and anti-Rab9 (Cell Signaling); anti-actin (Sigma); anti-pericentrin and anti–cation-independent mannose-6-phosphate receptor (CI-MPR) (Abcam); and anti-perforin (Mabtech, BioLegend, or Cell Sciences).

Cells

YTS, 721.221, and 293T cells were grown as described previously.[16] YTS cells, transduced with short hairpin RNA (shRNA), were grown in complete RPMI 1640 medium with puromycin (2 μg/mL). NK92 cells were cultured in RPMI 1640 medium with interleukin 2 (IL-2) (100 U/mL). Blood samples from healthy volunteers were collected at the Department of Transfusion Medicine, National Institutes of Health (NIH), under protocol 99CC-0168, and used to isolate NK cells. NK cells were cultured in X-vivo medium (Invitrogen) supplemented with 500 U/mL of IL-2.

RNAi constructs

LAMP1 and adaptin γ short interfering RNA (siRNA) or vector-based shRNA was from Sigma. For YTS cells, nontargeting shRNA (Sigma) was used as a negative control, whereas for ex vivo NK cells, a scrambled siRNA was used. Both nontargeting shRNA and scrambled siRNA are collectively referred to as control (CTRL) RNA interference (RNAi). Generation of lentivirus particles and infection of YTS cells was done as described by Krzewski et al.[16] siRNA was delivered to ex vivo isolated NK cells by nucleofection using Nucleofector II (Lonza), and the cells were analyzed 72 hours after the procedure.

RNA isolation, reverse transcription–polymerase chain reaction (PCR), quantitative PCR, and western blotting

Total RNA was isolated with RNAqueous-4PCR kit (Ambion). Complementary DNA (cDNA) was generated with qScript cDNA Synthesis Kit (Quanta) and served as template for real-time PCR, using SYBR Green Master Mix and LightCycler 480 (Roche). Primers for real-time PCR were from Qiagen. The amount of the target gene messenger RNA (mRNA) was calculated from the standard curve and normalized to actin mRNA.

For immunoblotting, cell lysates or cell fractions were probed with the Ab's indicated in the text. Immunoblots were developed using ChemiGlow West Substrate (Cell Biosciences). The images were acquired with FluorChem-Q imager (Protein Simple), using AlphaView (version 3.3) and automatic exposure.

Cytotoxicity assay

NK-cell cytotoxicity was evaluated by Dissociation-Enhanced Lanthanide Fluorescent Immunoassay (Perkin-Elmer). Lysis percentage was calculated as described by Krzewski et al.[16]

Flow cytometry

YTS or NK cells were fixed, permeabilzed with Cytofix/Cytoperm buffer (BD), and stained with anti-LAMP1–fluorescein isothiocyanate, anti-LAMP2–AlexaFluor 647, and/or anti-perforin Ab, conjugated to fluorescein isothiocyanate or phycoerythrin.

Delivery of granzyme B to 721.221 target cells was assessed using GranToxiLux kit (OncoImmunin). In this assay, target cells are labeled with a cell-permeable fluorogenic granzyme B substrate; upon delivery of granzyme B to the target cell, the substrate is cleaved resulting in increased fluorescence in target cells.[26] Data acquisition and analysis were done using FACSort (BD) and FlowJo (version 7.6; Tree Star).

Granzyme B activity

Activity of granzyme B in cell lysates was assessed according to Thiery et al.[27]

Cell conjugation

The assay was performed as described in Krzewski et al.[16]

Microscopy and image analysis

YTS cells were conjugated to 721.221 target cells at a 1:1 ratio at 37°C. Fixed and permeablized cells were stained with the Ab's indicated in text. For the double staining of perforin, the cells were first stained with anti-perforin B-D48 Ab, followed by IgG1-specific DyLight 549–conjugated anti-mouse Ab, blocked with 5% mouse serum, and stained with directly conjugated anti-perforin δG9 Ab. Cells were visualized by a Zeiss LSM510 Axiovert-200M confocal microscope at room temperature. The images were obtained using 63× Plan-Apochromat objective and LSM510 (version 3.2).

The determination of characteristics of perforin clusters and colocalization analysis were done using ImageJ (version 1.45; NIH) and Imaris (version 7.3; Bitplane), respectively, as described in the supplemental Methods.

For live cell imaging, YTS cells were labeled for 30 minutes with 75 nM LysoTracker Red DND-99 (Invitrogen) and placed in Laboratory-Tek chambered coverglass (Nunc) in phenol-red free RPMI. Cells were imaged in all 3 planes for 3 minutes at 37°C using an Olympus IX81 microscope with 100× PlanApo objective. Image acquisition was performed with MetaMorph (version 7.7.3; Molecular Devices) using 0.5-μm z-axial dimension and 100-millisecond exposure/frame. Three-dimensional vesicle tracking was done using Imaris, using an estimated diameter of 0.3 μm, autoregressive motion tracking algorithm, 1.5 maximum distance, 3 maximum gap size, and track duration >2 seconds; track speed was calculated as the average speed of granule movement during the imaging period.

Granule isolation and cell fractionation

YTS cells were homogenized using Dounce homogenizer. Cell debris and nuclei were pelleted (1000g_{av}, 10 minutes), and the postnuclear supernatant was centrifuged (17 000g_{av}, 15 minutes) to pellet the crude lysosomal fraction (CLF). The CLF was adjusted to 25% iodoxanol. Ten percent to 40% discontinuous gradient of iodoxanol was centrifuged for 2 hours at 95 000g_{av}. In fractionation experiments, the postnuclear supernatants were overlaid on top of a 5% to 30% gradient of iodoxanol. The gradient was centrifuged at 52 000g_{av} for 18 hours.

Results

LAMP1 silencing results in inhibition of NK-cell cytotoxicity

To investigate the role of LAMP1 in NK-cell function, we evaluated the effect of LAMP1 silencing on NK-cell cytotoxicity. We generated YTS and NK92 NK cell lines with a stable LAMP1 knockdown (Figure 1A-B; supplemental Figure 1). Based on densitometric analysis of anti-LAMP1 immunoblotting, the estimated efficacy of LAMP1 knockdown was ~75%. With siRNA-mediated silencing of LAMP1 in ex vivo isolated IL-2–cultured human NK cells, we achieved a 40% to 50% decrease of LAMP1 protein. The lower LAMP1 knockdown level achieved in the transiently siRNA-transduced ex vivo NK cells was at least partially due to the stability of LAMP1; LAMP1 has a half-life of at least 30 hours, and the time point at which NK cells were analyzed (72 hours) was likely too short for stronger or full silencing of LAMP1 (supplemental Figure 2). LAMP1 RNAi had no effect on LAMP2 mRNA levels (supplemental Figure 3), confirming the specificity of RNAi.

We used LAMP1 RNAi cells to assess their ability to kill a tumor cell line, 721.221 or K562 (Figure 1C; supplemental Figure 1). We found that compared with untransduced YTS cells, or cells transduced with nontargeting control RNAi, LAMP1 RNAi cells had a 70% to 76% decrease in cytotoxicity. Likewise, LAMP1

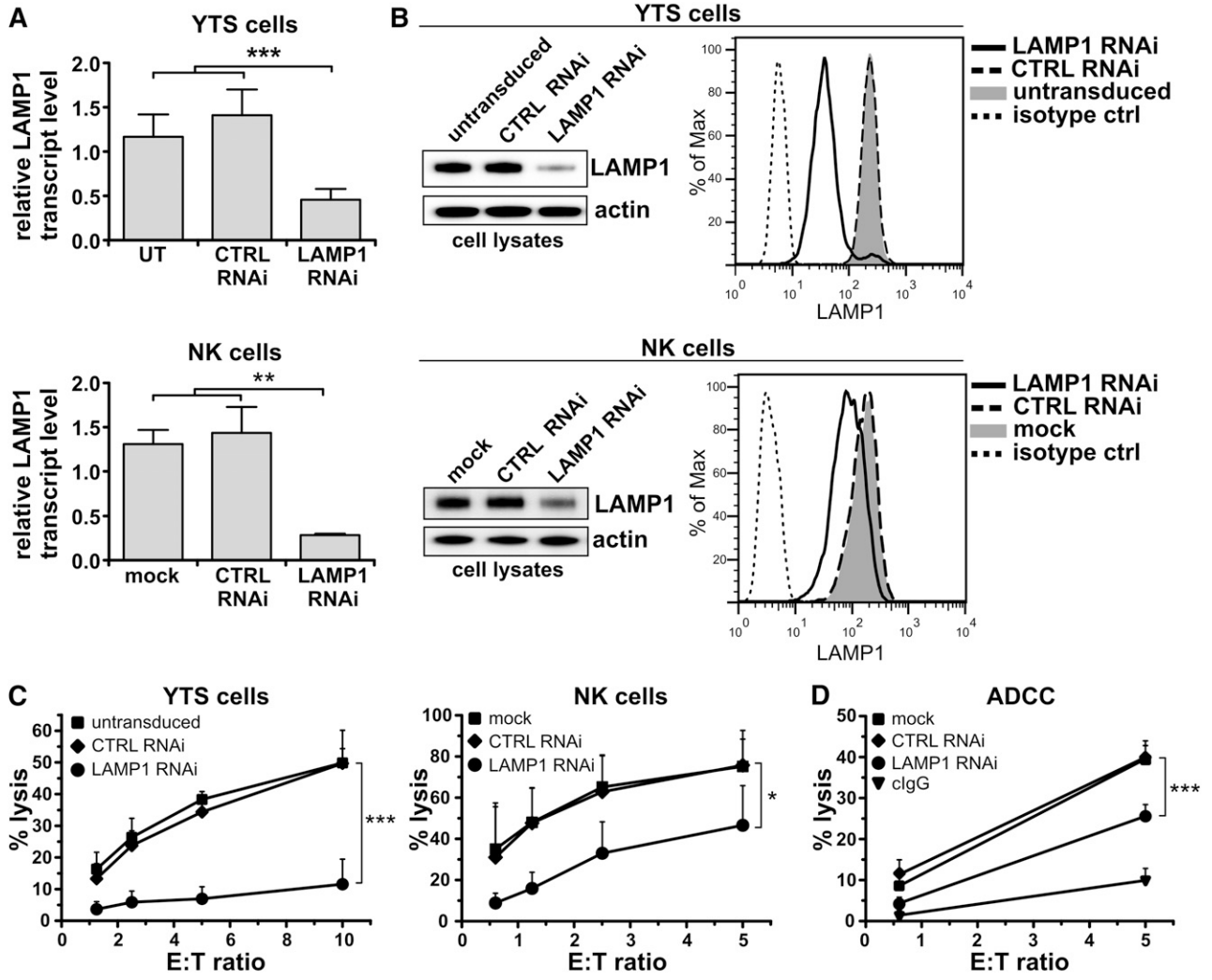

Figure 1. Disruption of LAMP1 expression inhibits cytotoxic activity of NK cells. (A) YTS (top) or ex vivo isolated NK cells (bottom) were untransduced (UT; YTS cells), mock-transduced (mock; NK cells), or transduced with control (CTRL) or LAMP1 RNAi. Levels of LAMP1 transcripts in the indicated cells were analyzed by real-time PCR; relative expression of LAMP1, normalized to actin, is shown. Data are represented as mean + standard deviation (SD) from 6 (YTS) or 3 (NK) analyses. $^{**}P < .01$; $^{***}P < .001$; one-way analysis of variance (ANOVA). (B) Protein level of LAMP1 in the indicated cells was analyzed by western blot (left; actin was used as a loading control) and by flow cytometry (right). (C) Cytotoxic activity of YTS and NK cells, untransduced, mock-transduced, or transduced with CTRL or LAMP1 RNAi. The percentages of 721.221 target-cell lysis for different effector-to-target (E:T) ratios are shown as mean values + SD determined from at least 5 experiments. $^{*}P < .05$; $^{***}P < .001$; 2-way ANOVA. (D) Ab-dependent cell-mediated cytotoxicity. Ex vivo isolated NK cells, either mock-transduced or transduced with CTRL or LAMP1 RNAi, were incubated with SK-OV3 target cells, in the presence of either human IgG (negative control) or anti-HER2 Ab. The percentage of target-cell lysis was determined from 3 experiments with different donors and is shown as means + SD. $^{***}P < .001$; 2-way ANOVA.

silencing decreased the cytotoxicity of NK92 cells by ~65%. We obtained similar results using ex vivo isolated NK cells, where a transient knockdown of LAMP1 reduced cytotoxicity by 40% to 60%. We also used Ab-dependent cell-mediated cytotoxicity to evaluate the killing ability of LAMP1 RNAi NK cells (Figure 1D). Although CD16-mediated recognition of anti-Human Epidermal Growth Factor Receptor 2 (HER2) Ab, bound to the cell surface of SK-OV3 cells, resulted in pronounced lysis of target cells by control-transduced NK cells, cytotoxicity by LAMP1 RNAi NK cells was decreased by 35% to 40%. Thus, LAMP1 plays an important role in NK-cell cytolytic activity.

Impaired delivery of granzyme B from LAMP1 RNAi cells to target cells

NK cells kill target cells by secreting granzyme-containing lytic granules at the immunologic synapse. We measured the ability of LAMP1 RNAi NK cells to deliver granzyme B to target cells. The delivery of granzyme B from LAMP1 RNAi YTS cells to target cells was decreased fivefold when compared with untransduced or control RNAi-transduced YTS cells (Figure 2A). We verified these results in NK cells, where LAMP1 silencing blocked the transfer of granzyme B from IL-2–stimulated NK to tumor cells almost twofold (Figure 2A). The smaller effect observed in the case of ex vivo NK cells was likely due to less efficient knockdown of LAMP1 in these cells and was consistent with the results of cytotoxicity assays. LAMP1 RNAi cells had normal levels of granzyme B (Figure 2B), and the activity of granzyme B from LAMP1 RNAi cells was undistinguishable from the activity observed in control cells (Figure 2C). LAMP1 RNAi cells formed conjugates with target cells at the same level as control cells (Figure 2D), excluding the possibility that blockage of granzyme B delivery and cytotoxicity resulted from inadequate cell-cell adherence. LAMP1 silencing did not affect the expression of NK-activating receptors on the cell

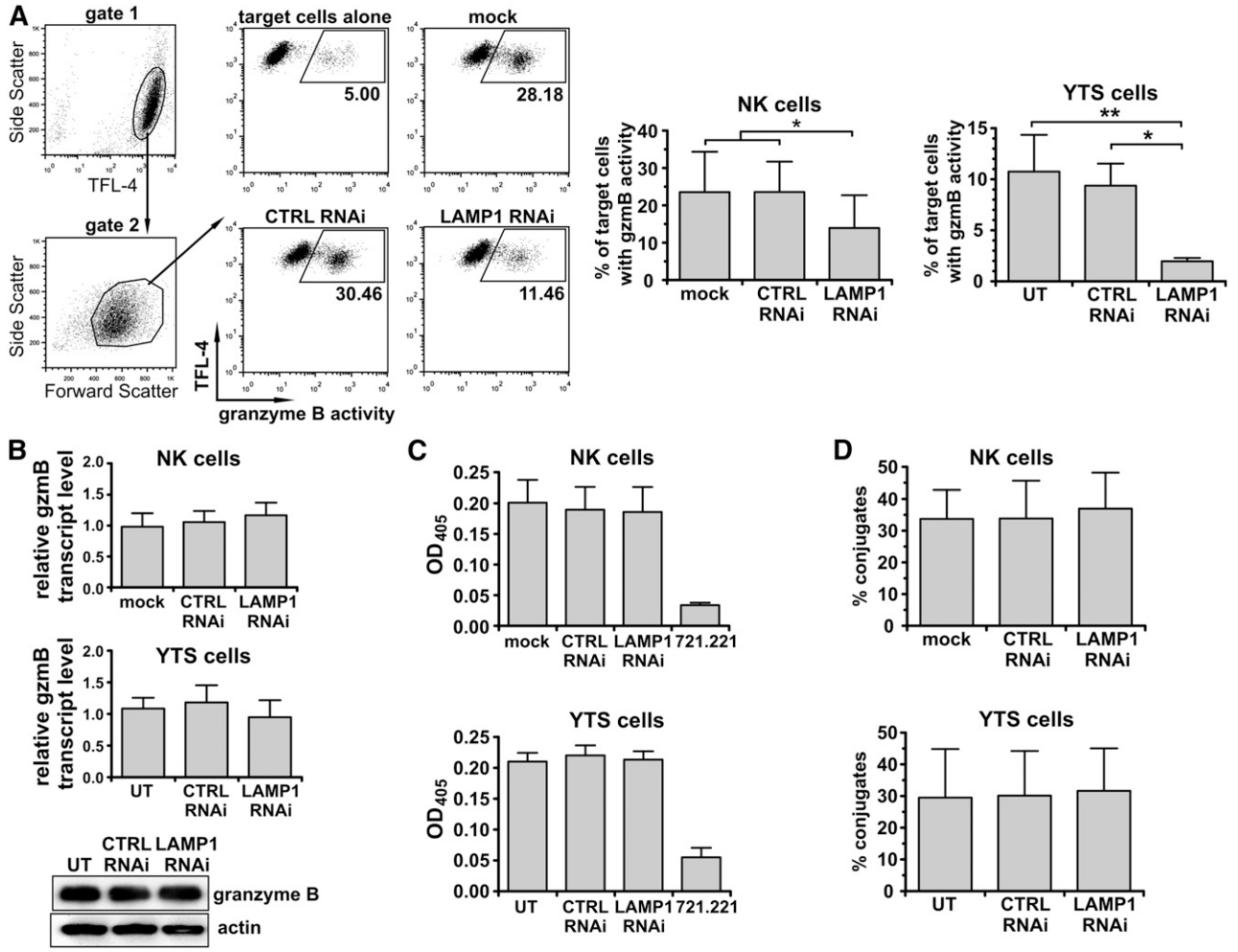

Figure 2. Delivery of granzyme B to target cells, but not cell-cell conjugation, is impaired in LAMP1 RNAi cells. YTS or ex vivo isolated NK cells were untransduced (UT; YTS cells), mock-transduced (mock; NK cells), or transduced with control (CTRL) or LAMP1 RNAi. (A) Delivery of granzyme B to target cells. The 721.221 target cells were labeled with TFL-4 and a fluorogenic substrate of granzyme B and then mixed with NK cells for 30 minutes at 37°C. The increase of substrate fluorescence in TFL-4–positive target cells, indicating the activity of granzyme B, was monitored by flow cytometry. The dot plots show gating strategies used and illustrate an example of the results for primary NK cells. Graphs (right) show mean values + SD determined from 5 (NK) or 3 (YTS) experiments. $*P < .05$; $**P < .01$; 1-way ANOVA. (B) Levels of granzyme B. Granzyme B transcript levels for YTS and primary NK cells were analyzed by real-time PCR. Relative expression of granzyme B, normalized to actin, is shown as mean + SD from 3 (NK) or 6 (YTS) experiments. Granzyme B protein level in YTS cells was visualized by western blotting; actin was used as a loading control. (C) Granzyme B activity. YTS or primary NK cells were lysed, and the proteolytic activity of granzyme B in total cell lysates was determined by measuring the hydrolysis of the peptide substrate. The graphs show mean values + SD from 5 (NK) or 3 (YTS) experiments. Granzyme B–negative 721.221 cells served as a control. (D) Cell conjugation. YTS or primary NK cells were stained with 5-chloromethylfluorescein diacetate (CMFDA) and mixed with TFL-4–labeled 721.221 target cells for 30 minutes at 37°C. Cells were then fixed and analyzed using flow cytometry. Conjugates of NK and target cells were determined by measuring the percentage of CMFDA+TFL-4+ double-positive cells from the total pool of live CMFDA+ cells. The mean values + SD were determined from 4 experiments.

surface; moreover, LAMP1-silenced cells accumulated Lymphocyte Function-associated Antigen 1 and filamentous actin, essential for NK-cell activation and cytotoxicity, at the immunologic synapse similar to nonsilenced cells, demonstrating that the synapse formation and NK-cell activation was likely not impaired in those cells (supplemental Figure 4). Following the stimulation with target cells, LAMP1 RNAi cells were able to upregulate LAMP2 and LAMP3 (CD63) on the cell surface (albeit at a slightly lower frequency than the controls), indicating that the lytic granules were able to fuse with the plasma membrane (supplemental Figure 5).

LAMP1 silencing does not prevent polarization of lytic granules but affects perforin clustering at the cell-cell contact site

NK-cell cytotoxicity depends on the ability to transport their lytic granules to the immunologic synapse. Therefore, we next evaluated the granule transport to the cell-cell interface. As the results using YTS cells mimicked the data obtained with ex vivo NK cells, we used the YTS model to study the localization of perforin-containing lytic granules in response to activation with target cells.

LAMP1 RNAi cells translocated the lytic granules toward the immunologic synapse (Figure 3A). The microtubule organizing center (MTOC), as detected by pericentrin staining, was positioned close to the immunologic synapse, just as in control cells, indicating that the migration of the MTOC was not affected by LAMP1 silencing. There was no significant difference in perforin polarization (Figure 3B); however, perforin appeared to be more dispersed around the MTOC in LAMP1 RNAi cells (Figure 3A). The analysis of shapes of perforin-positive vesicle clusters revealed significant changes in shape descriptors. The main area occupied by perforin in LAMP1 RNAi cells had smaller solidity and circularity, indicating that with reduced levels of LAMP1, lytic granules did not form tight

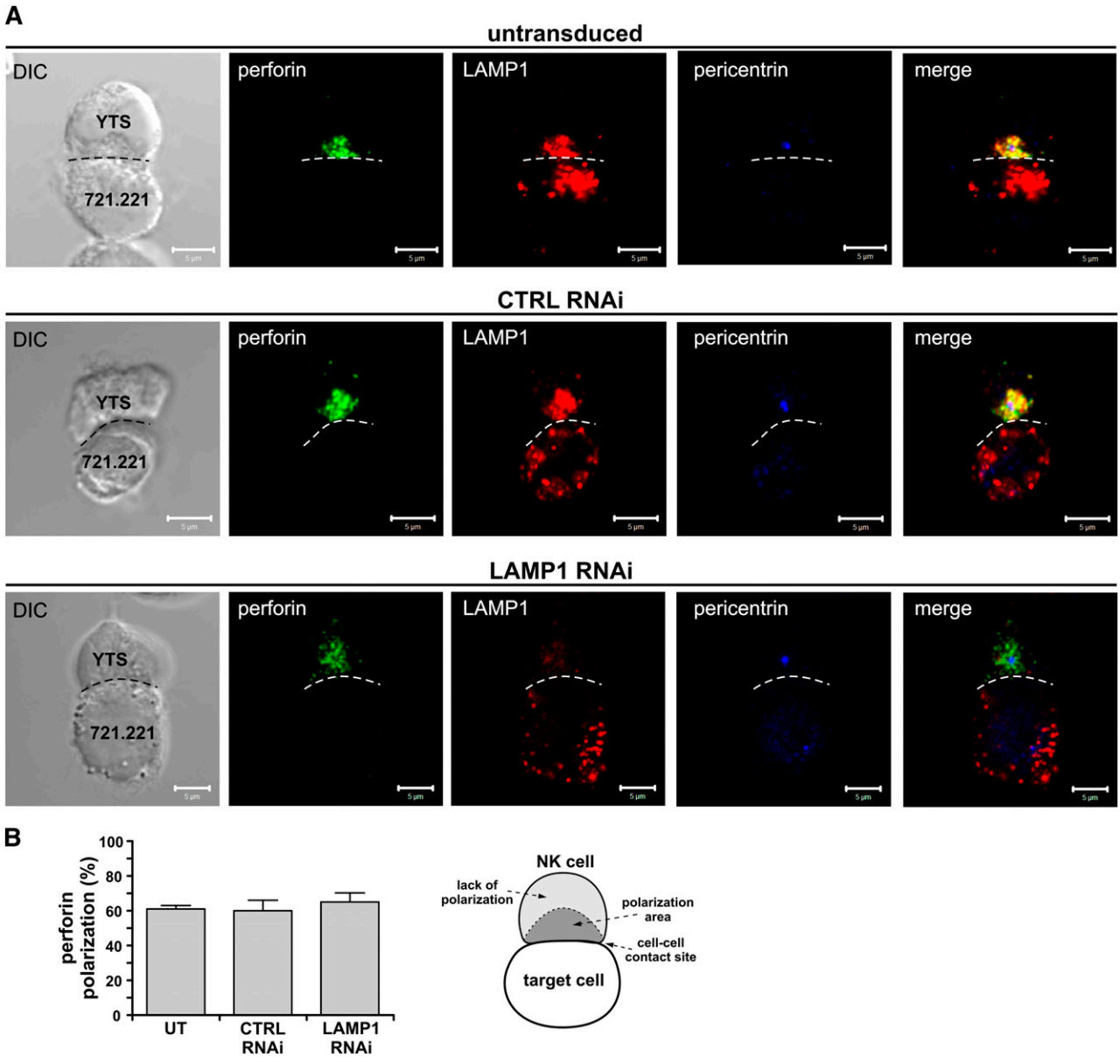

Figure 3. Effects of LAMP1 silencing on recruitment of perforin to the immunologic synapse. (A) YTS cells, untransduced or transduced with control (CTRL) or LAMP1 RNAi, were activated by mixing with 721.221 target cells for 30 minutes at 37°C. The cells were next fixed and stained with Ab's against LAMP1 (red), pericentrin (MTOC marker; blue), and perforin (green). The dashed line indicates the position of the immunologic synapse. Scale bars represent 5 μm. (B) The percentages of perforin polarization to the immunologic synapse in YTS cells conjugated with 721.221 target cells, as in (A). Error bars represent SD. The values were determined by evaluation of 150 conjugates for each indicated YTS cell group in 3 experiments. The diagram (right) illustrates the scoring model. Perforin was regarded as polarized if it localized to a conical area (dark gray region in the diagram labeled as polarization area), limited by the center of the cell and the edge points of the cell-cell interface (shown as the dashed line in the illustration), and the MTOC (as determined by pericentrin staining) was adjacent to the cell-cell contact site.

clusters and were more spread out (supplemental Figure 6). We also observed a dispersed distribution of lytic granules when using LAMP2 as another marker for the granules (not shown). Thus, although the MTOC and perforin are able to move toward the immunologic synapse in response to cell activation, the lytic granules remain dispersed and do not cluster efficiently in LAMP1 RNAi cells.

Impairment of lytic granule movement in LAMP1 RNAi cells

The previous results suggested a possible defect in granule transport in LAMP1 RNAi cells. Hence, we performed three-dimensional time-lapse imaging of LysoTracker-labeled lytic granules in live cells (supplemental Videos 1 and 2) and plotted the trajectories formed by moving vesicles. We found that granules in LAMP1 RNAi cells formed shorter tracks, with a smaller displacement (ie, the straight-line distance between the beginning and end of the track) and decreased velocity (Figure 4A-B).

The activity of the motor complex dynein-dynactin is essential for the movement of lytic granules toward the MTOC.[28] We isolated lytic granules from control and LAMP1 RNAi cells and determined the levels of the dynein/dynactin complex regulatory subunit, $p150^{glued}$. Cells with LAMP1 knockdown had less $p150^{glued}$ recruited to their lytic granules (Figure 4C). Rab7, directly involved in the recruitment of $p150^{glued}$, was present to the same extent on the granules from control and LAMP1 RNAi cells, suggesting that the decreased recruitment of dynactin is not related to changes in Rab7 levels. The

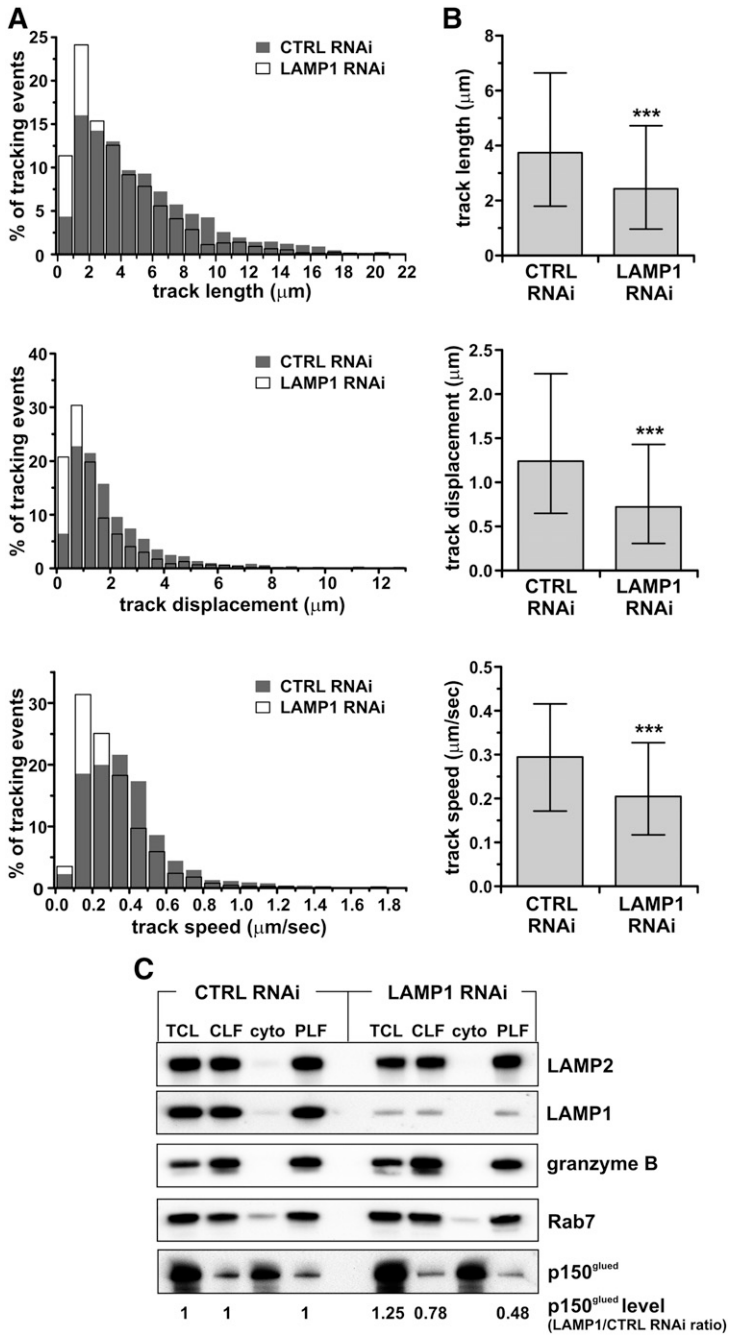

Figure 4. Impairment of lytic granule movement caused by LAMP1 deficiency. YTS cells, stably transduced with control (CTRL) or LAMP1 RNAi, were labeled with LysoTracker Red. The cells were visualized using spinning disk confocal microscopy, and the movement of LysoTracker-labeled vesicles was recorded in 3 dimensions (x-y-z plane) for 180 seconds. The characteristics of vesicle trajectories were derived from analysis of 10 (LAMP1 RNAi) or 11 (CTRL RNAi) cells in 3 experiments. (A) Histograms of frequency distributions of the length (top), displacement (the distance in straight line between the beginning and end of the track; middle), and mean velocity (bottom) of granule trajectories in CTRL and LAMP1 RNAi cells. (B) Graphs show the median values and interquartile range of the length, displacement, and velocity of granules from CTRL and LAMP1 RNAi cells. ***$P < .001$; Mann-Whitney U test. Granules in LAMP1 RNAi cells formed shorter tracks, with the majority (75%) in the range of 0.96 to 4.7 μm, whereas in CTRL RNAi cells the majority of tracks were in the range of 1.8 to 6.6 μm. The median track length in LAMP1 RNAi cells was 2.43 μm, and 3.74 μm in CTRL RNAi cells. The track displacement was also decreased in LAMP1 RNAi cells: 0.3 to 1.4 μm vs 0.65 to 2.2 μm in CTRL RNAi cells; the median displacement value was 0.72 μm and 1.24 μm in LAMP1 and CTRL RNAi cells, respectively. The majority of vesicles in LAMP1 RNAi cells moved at 0.12 to 0.33 μm/s, whereas in CTRL RNAi cells they moved in the range of 0.17 to 0.42 μm/s (in agreement with Mentlik et al[28]); the median speed was 0.2 μm/s in LAMP1 RNAi cells, compared with 0.29 μm/s in CTRL RNAi cells. (C) LAMP1 is required for proper recruitment of p150^{glued}/dynactin to lytic granules. YTS cells, transduced with either CTRL or LAMP1 RNAi, were homogenized, and their lytic granules were purified on a 10% to 40% discontinuous gradient of iodoxanol. The presence of proteins in the total cell lysate (TCL), CLF, cytoplasmic fraction (cyto), and purified lysosomal fraction (PLF) was assessed by immunoblotting with the Ab's specific for the indicated proteins; granzyme B and LAMP2 were used as loading controls. The result is representative of 2 separate experiments. The changes in p150^{glued} levels, normalized to LAMP2 levels, were calculated as the ratio between p150^{glued} band intensity from LAMP1 and CTRL RNAi cells in the appropriate samples (eg, p150^{glued} band intensity from LAMP1 RNAi cell PLF sample divided by the band intensity from CTRL RNAi cell PLF sample).

lysosome-specific proteins, granzyme B and LAMP2, were absent in cytoplasmic fractions but present in the lysosomal fractions at similar levels, verifying the purity of the lysosomal fractions and indicating that the observed loss of p150^{glued} was specific. Thus, LAMP1 silencing leads to lytic granule movement impairment, likely due to the decreased recruitment of motor protein(s) to the granules.

LAMP1 silencing affects perforin trafficking and leads to decreased perforin level in the lytic granules

As the altered rate of lytic granule transport in LAMP1 RNAi cells was likely not sufficient to fully block their cytolytic capacity, we explored if other factors could account for the reduced cytotoxicity. During imaging studies, we observed that LAMP1 RNAi cells had weaker anti-perforin staining (Figure 3A), suggesting that these cells could have less perforin. Reconstruction of multiple optical sections of YTS cells stained with anti-perforin Ab (Figure 5A) confirmed that, in addition to the greater dispersion of perforin-containing granules, the anti-perforin staining was much weaker in LAMP1 RNAi than in control cells. The fluorescence of perforin clusters was decreased by ~35% when compared with untransduced or control RNAi cells (Figure 5B). Flow cytometry analysis revealed a 40% decrease in perforin level in LAMP1-silenced YTS cells when compared with control cells; we obtained similar results using ex vivo isolated IL-2–stimulated NK cells (Figure 5C). This difference was observed only at the protein level, as perforin mRNA was not affected by LAMP1 silencing (Figure 5D), and did not result from protein degradation, as the half-life of perforin was comparable between control and LAMP1 RNAi cells (supplemental Figure 2).

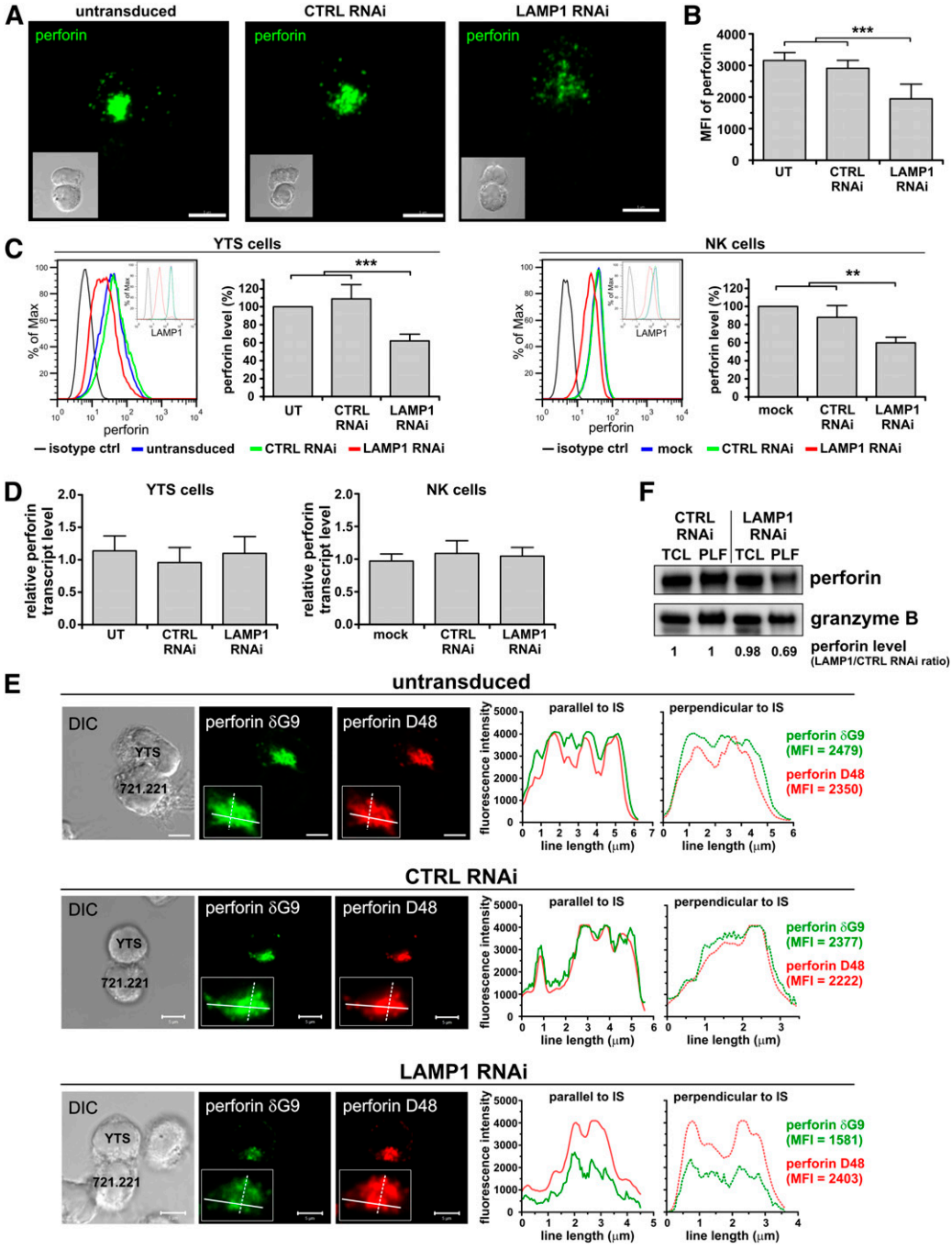

Figure 5. Disruption of LAMP1 expression results in decreased association of perforin with lytic granules. YTS or ex vivo isolated NK cells were untransduced (UT; YTS cells), mock-transduced (mock; NK cells), or transduced with control (CTRL) or LAMP1 RNAi. (A) Visualization of perforin in cells. YTS cells were mixed with 721.221 target cells for 30 minutes at 37°C. The cells were fixed and stained with anti-perforin δG9 Ab. Multiple optical sections were acquired every 0.3 μm in order to visualize all the perforin in the cell. The images show two-dimensional reconstruction of overlaid optical sections of the indicated transduced YTS cells interacting with the target cells. Inserts show differential interference contrast (DIC) images of the conjugated cells (YTS cell is depicted above the target cell). Scale bars represent 5 μm. (B) The summary of perforin fluorescence intensity quantification. Perforin in YTS cells was visualized by staining with anti-perforin δG9 Ab. The intensity of main perforin cluster (as defined in the supplemental Methods and supplemental Figure 3) was measured and plotted as mean + SD. The data were determined in 2 experiments by analyzing the following cell numbers: UT, n = 21; CTRL RNAi, n = 12; LAMP1 RNAi, n = 25 cells. (C) Intracellular levels of perforin. YTS or NK cells were fixed, permeabilized, stained with anti-perforin δG9 Ab and analyzed using flow cytometry. Representative histograms of perforin staining by flow cytometry (left; inserts show the protein level of LAMP1), whereas the graphs (right) summarize mean values + SD of the median perforin fluorescence from 4 (NK) or 7 (YTS) experiments. The perforin level in mock-transduced or untransduced cells was regarded as 100%, and the changes in perforin level in relation to the mock-transduced or untransduced cells are indicated for CTRL and LAMP1 RNAi cells. Asterisks in (B) and (C) indicate statistical significance: $^{**}P < .01$; $^{***}P < .001$; 1-way ANOVA. (D) Perforin mRNA levels. Transcripts of perforin in the indicated cells were measured by real-time PCR; relative expression of perforin, normalized to actin, is shown. Data are represented as mean values + SD from 4 or 7 experiments, using NK and YTS cells, respectively. (E) Decreased levels of lysosomal perforin in cells with LAMP1 knockdown. The indicated YTS cells were mixed with 721.221 cells for 30 minutes at 37°C. The cells were fixed, stained with anti-perforin D48 Ab followed by DyLight 549–conjugated isotype specific anti-mouse Ab (red), and then stained with Alexa Fluor 488–conjugated anti-perforin δG9 Ab (green). The inserts show close-ups of perforin polarized to the cell-cell contact area. The plots (right) show profiles of the fluorescence intensity of anti-perforin staining using δG9 or D48 Ab, measured along the lines drawn across the widest area parallel or perpendicular to the cell-cell contact site and indicated in the inserts of the images. Scale bars represent 5 μm. (F) Perforin level in TCL or PLF from YTS cells transduced with CTRL or LAMP1 RNAi was analyzed by western blot (using anti-perforin Pf-344 Ab). Anti–granzyme B immunoblotting was used as a loading control. The result is demonstrative of 3 experiments. The changes in perforin levels, normalized to granzyme B levels, were calculated as the ratio between perforin band intensity from LAMP1 and CTRL RNAi cells in the appropriate sample, as described in Figure 4C.

The Ab used for perforin detection (clone δG9) reportedly recognizes the mature, lysosomal form of perforin.[29,30] Another anti-perforin Ab, D48, has been described to detect multiple forms of perforin (ie, newly synthesized as well as lysosomal).[29-31] Therefore, we used these 2 Ab's to determine if LAMP1 silencing affects the total amount or only the granule-associated perforin in the cell. Perforin staining with δG9 Ab showed that fluorescence of granule-contained perforin was decreased following LAMP1 knockdown, whereas the fluorescence profiles of anti-perforin staining using D48 Ab were virtually the same (Figure 5E; supplemental Figure 7). Additionally, granules isolated from LAMP1 RNAi cells had a similar level of granzyme B but less perforin than granules from control RNAi cells, whereas the amount of total perforin in cell lysates did not differ (Figure 5F).

The loss of granule-associated perforin could result from its missorting, leading to increased secretion or trapping of perforin in nonlysosomal compartments. We were unable to detect any changes in the amount of perforin released to the cell culture supernatants (not shown), indicating that perforin is likely not prematurely secreted from cells after LAMP1 silencing. To address the second possibility, we analyzed cell fractionations for perforin content. In control and LAMP1 RNAi cells, the distribution of markers for several cellular organelles (EEA-1, Rab9, Rab7, and LAMP2) was the same (Figure 6A). Granzyme B was present in fractions positive for Rab7 and LAMP2, indicating that following LAMP1 knockdown granzyme B is properly sorted into lysosomes. In control RNAi cells, the majority of perforin was present in the fractions containing lysosomal markers. In LAMP1 RNAi cells, however, some perforin localized to lesser density fractions negative for LAMP2, granzyme B, or Rab7/9, demonstrating that in the absence of LAMP1, perforin does not traffic properly to lysosomes and is partially retained in nonlysosomal compartments. The nonlysosomal fractions positive for perforin in LAMP1 RNAi cells were also positive for 1 of the 2 MPR forms and overlapped with adaptin γ (Figure 6A), suggesting that in these cells perforin could be accruing in *trans*-Golgi network (TGN)–derived transport vesicles. To verify this hypothesis, we analyzed colocalization between perforin and MPR in YTS cells with normal or reduced LAMP1 expression.

Although the lysosomal perforin (δG9-reactive) minimally overlapped with MPRs (supplemental Figure 8A-B), the staining with D48 anti-perforin Ab showed evident colocalization with CI-MPR (Figure 6B). In control RNAi cells, 23% of perforin overlapped with CI-MPR, whereas 40% of perforin colocalized with CI-MPR in LAMP1 RNAi cells (Figure 6C). The overlap coefficient between perforin and CI-MPR was also significantly increased in cells with LAMP1 knockdown when compared with control cells (Manders coefficient M = 0.4 vs 0.21, respectively). LAMP1 was also found to partially colocalize with CI-MPR (supplemental Figure 8C). More perforin-positive vesicles were also positive for adaptin γ, and negative for LAMP2 in LAMP1 RNAi cells (supplemental Figure 9 and data not shown), further supporting the idea that without LAMP1, perforin is retained in transport vesicles and does not reach the lytic granules. The defect in perforin trafficking was not due to a general impairment of the protein transport, as the cell surface expression of NK-cell receptors and the ability of NK cells to secrete tumor necrosis factor α and interferon γ were not significantly affected by LAMP1 silencing (supplemental Figures 4A and 10). Thus, disruption of LAMP1 expression alters perforin trafficking and causes retention of perforin in transport vesicles, resulting in decreased perforin content in lytic granules.

Silencing of adaptin γ also causes retention of perforin in transport vesicles

The adaptor protein complex AP-1, important for sorting proteins leaving the TGN, is known to directly interact with LAMP1.[32] Therefore, we analyzed the effect of silencing the AP-1 complex subunit, adaptin γ, on perforin location in YTS cells. Adaptin γ silencing resulted in increased association of perforin with MPR-positive vesicles (Figure 7A). In adaptin γ RNAi cells, ~51% of perforin overlapped with CI-MPR, whereas only 21% overlapped in control RNAi cells (Figure 7B). The overlap coefficient increased from 0.16 in control RNAi cells to 0.39 in adaptin γ RNAi cells. Adaptin γ knockdown had a similar effect on cytotoxicity as the silencing of LAMP1 (Figure 7C). Thus, disruption of AP-1 complex expression also causes retention of perforin in transport vesicles and produces effects similar to LAMP1 silencing, indicating that these 2 binding partners are important for proper trafficking of perforin to lytic granules and NK-cell cytotoxicity.

Discussion

Although recent reports have highlighted the role of several proteins involved in lytic granule transport and exocytosis,[12-16,33] the function of granule-specific proteins in NK-cell cytotoxicity is poorly characterized. Here, we investigated the role of the lytic granule protein LAMP1 in the cytotoxicity of NK cells. We found that LAMP1 silencing resulted in inhibition of NK-cell cytotoxicity, demonstrating for the first time the importance of LAMP1 in this process.

In order to kill, NK cells must first translocate the MTOC and polarize their lytic granules toward the cell-cell contact site, a step that is required for the subsequent release of lytic granule content at the immunologic synapse.[2,3] YTS NK cells were able to form immunologic synapses, and move their MTOC and granules toward the immunologic synapse, regardless of the level of expression of LAMP1; contrary to cells with normal expression of LAMP1, in LAMP1 RNAi cells the granules were more dispersed and did not form thick clusters. This finding is consistent with a previous report showing that lysosomes in *lamp1/lamp2*-deficient mouse fibroblasts have severely reduced motility, supporting the hypothesis that LAMPs are involved in the transport of lysosomes.[24] Our analysis of the spatiotemporal movement of LysoTracker-labeled granules revealed that the reduction of LAMP1 expression is sufficient to disturb motility of lysosomes in NK cells and likely contributes to decreased cytotoxicity. The contribution of LAMP2 to lytic granule movement in NK cells is unknown, but the endogenous LAMP2 appears unable to fully compensate for defects in lysosomal movement caused by LAMP1 silencing.

Trafficking of lytic granules in NK cells depends on the activity of minus end–directed motor protein complex dynein-dynactin.[28] We found that lytic granules isolated from cells with LAMP1 knockdown had less $p150^{glued}$; the decreased recruitment of motor protein to lytic granules could explain the defect in granule movement caused by LAMP1 silencing. Interestingly, we found that the presence of Rab7, responsible for recruiting dynactin-dynein to lysosomes and endosomes,[34,35] was unaffected by LAMP1 knockdown, indicating that the LAMP1-mediated effect is independent of Rab7. Recruitment of dynein-dynactin to Rab7 is not sufficient to activate the motor complex, and dynein-dynactin has to be transferred from Rab7 to βIII spectrin to initiate transport of

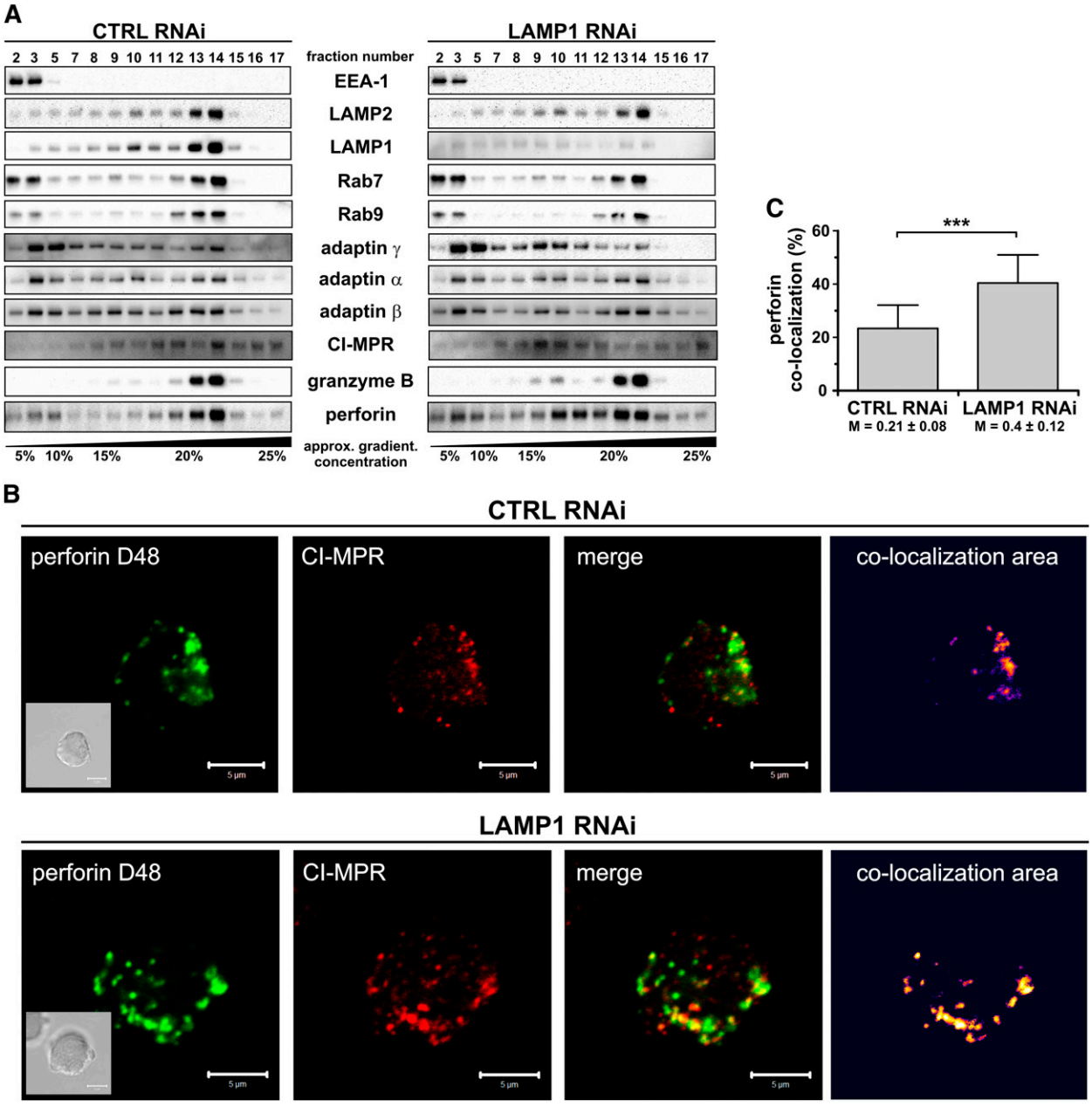

Figure 6. LAMP1 is required for efficient delivery of perforin, but not granzyme B, to lytic granules. (A) YTS cells, transduced with CTRL or LAMP1 RNAi, were homogenized and fractionated on a continuous 0% to 30% gradient of iodoxanol. The presence of the indicated proteins in the gradient fractions was assessed by immunoblotting; only relevant fractions are shown. The data are representative of 3 experiments. EEA-1 was used as a marker of early endosomes; Rab9, late endosomes; Rab7, late endosomes/lysosomes; and LAMP2, lysosomes. Adaptin γ and MPR were used as markers of TGN-derived transport vesicles. (B) YTS cells were fixed, stained with anti–CI-MPR Ab followed by DyLight 649–conjugated anti-mouse Ab (red), and then stained with Alexa Fluor 488–conjugated anti-perforin D48 Ab (green). The area of colocalization between the 2 fluorophores is shown as a heat map image. Scale bars represent 5 μm. Inserts show DIC images. (C) The percentage of colocalization between perforin (D48-reactive) and CI-MPR. The data were determined by analysis of 34 to 35 cells, as described in (B), and are shown as mean values + SD from 2 experiments. The numbers below the graph are Manders overlap coefficients ± SD. ***$P < .001$; Mann-Whitney U test.

vesicles.[34] Whether LAMP1 could be involved in this process and/or directly bind dynein-dynactin or other motor proteins is unknown at present. The cytoplasmic tail of LAMP1 is very short and, with the exception of a lysosome-sorting sequence, lacks clearly defined signaling motifs. There is a paucity of information regarding binding partners of LAMP1, and we are analyzing the proteins that interact with LAMP1 to determine how LAMP1 could be involved in motor protein recruitment to lytic granules.

We found that disruption of LAMP1 expression not only slowed granule movement, but also interfered with perforin recruitment to lytic granules. Lysosomal membrane proteins are known to be important for sorting lysosome luminal proteins, and disruption of their function can result in secretion of lysosomal enzymes instead of sorting to lysosomes. For instance, deficiency of the lysosomal integral membrane protein 2 results in premature secretion of β-glucocerebrosidase.[36] We did not find any evidence of increased release of perforin from NK cells, even though LAMP1 silencing caused an alteration in perforin trafficking. The distribution of EEA-1, LAMP2, Rab7, and Rab9 was the same between cells with normal and reduced expression of LAMP1, indicating that the endolysosomal

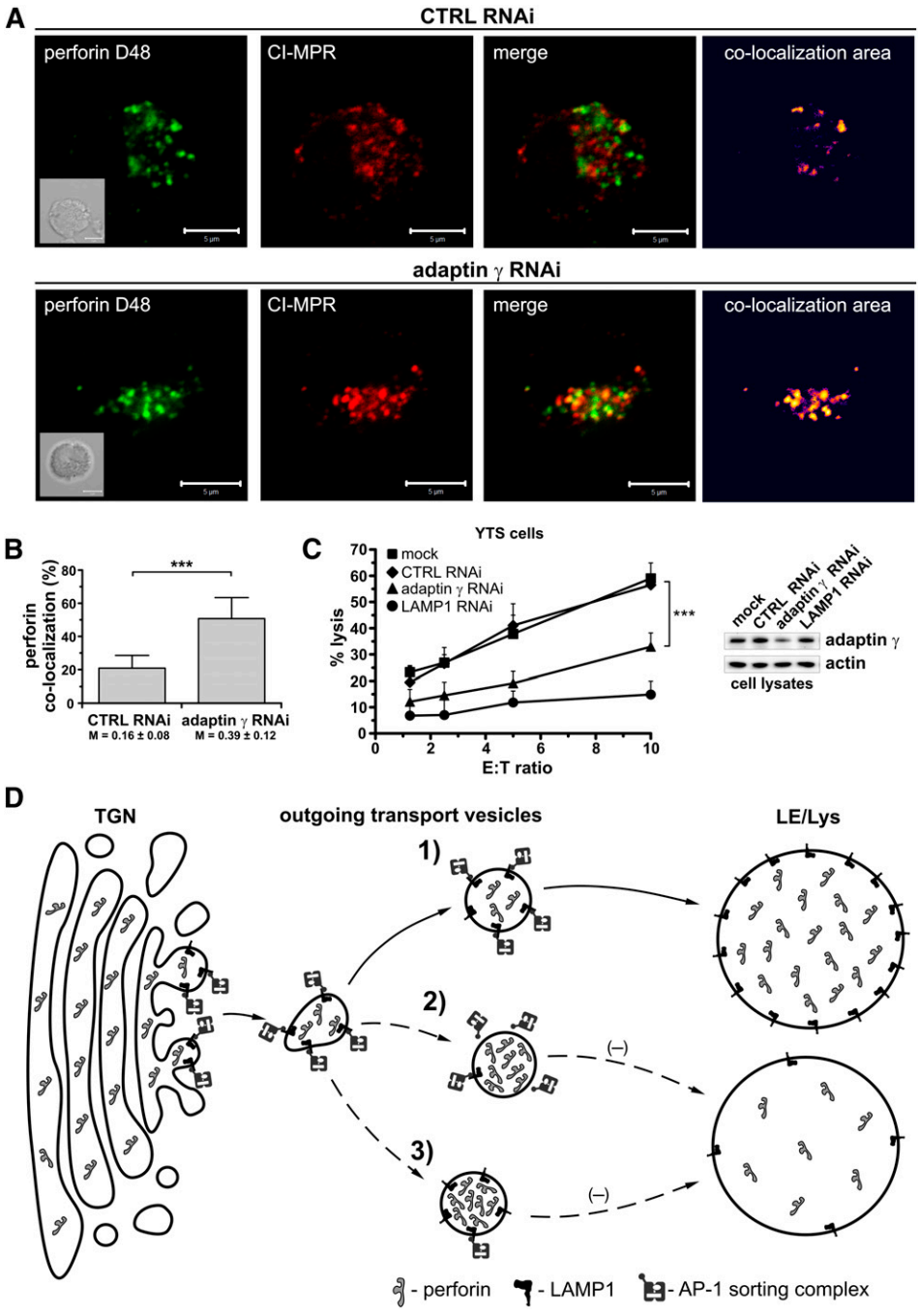

Figure 7. Silencing of adaptin γ causes retention of perforin in transport vesicles and blocks cytotoxicity. (A) YTS cells, transduced with CTRL or adaptin γ RNAi, were fixed, stained with anti–CI-MPR Ab followed by AlexaFluor 568–conjugated anti-mouse Ab (red), and then stained with Alexa Fluor 488–conjugated anti-perforin D48 Ab (green). The area of colocalization between the 2 fluorophores is shown as a heat map image. Scale bars represent 5 μm. Inserts show DIC images. (B) The percentage of colocalization between perforin (D48-reactive) and CI-MPR. The data were determined by analysis of 20 (CTRL RNAi) or 39 (adaptin γ RNAi) cells and are represented as mean values + SD from 2 experiments. The numbers below the graph show Manders overlap coefficients ± SD. ***$P < .001$; Mann-Whitney U test. (C) Cytotoxic activity of YTS cells, mock-transduced or transduced with CTRL, adaptin γ, or LAMP1 RNAi. The graph shows the percentage of 721.221 target-cell lysis at different E:T ratios and illustrates mean values + SD from 3 independent experiments. The image (right) shows the result of immunoblotting with anti–adaptin γ or anti-actin (loading control) Ab's in the indicated cells. (D) A model of LAMP1 function. The proteins destined for the lysosomes, such as perforin, leave the TGN in the outgoing transport vesicles and reach their destination due to the action of AP sorting complexes. In normal conditions (1), the AP-1 sorting complex recognizes and binds LAMP1 on the surface of the outgoing vesicles, allowing for transport of the LAMP1-positive, perforin-containing vesicles to the late endosomal/lysosomal (LE/Lys) compartment. Therefore, disrupting the interaction between LAMP1 and AP-1 would negatively affect perforin trafficking to the lysosomes. Silencing of LAMP1 (2), for example, would remove the AP-1 binding partner from the surface of the transport vesicles, preventing binding of AP-1 and causing retention of perforin in those vesicles. Consequently, less perforin would reach the lysosomes/lytic granules. Similarly, silencing of adaptin γ (and subsequent disruption of AP-1 expression) (3) would inhibit vesicle sorting, leading to the accumulation of the perforin-containing transport vesicles and decreased level of perforin in the secretory lysosomes.

system was not disturbed following LAMP1 knockdown; this agrees with a previous report showing that LAMP1-deficient cells have normal lysosomal morphology.[22] We found, however, that whereas the distribution of granzyme B was unchanged in LAMP1 RNAi cells, a pool of perforin was present in compartments that were negative for protein markers of late endosomes and lysosomes, indicating that perforin was retained in nonlysosomal structures in these cells. The nonlysosomal fractions containing perforin were positive for markers associated with vesicle transport and sorting, and we found increased colocalization of perforin with CI-MPR in LAMP1 RNAi cells, suggesting that perforin is present in *trans*-Golgi–derived transport vesicles. The presence of perforin in MPR-positive vesicles is somewhat surprising, as perforin has been reported to lack mannose-6-phosphate modification.[37] On the other hand, lysosomal proteins are able to use MPR-positive carrier vesicles even though they do not have the modification; for example, neuraminidase uses the interaction with mannose-6-phosphate–modified cathepsin A to reach lysosomes.[38] Concurring with our findings, a recent report demonstrating the importance of perforin glycosylation in its traffic to lytic granules postulates that perforin primarily uses the MPR-dependent pathway to reach lytic granules.[39]

Regardless of the trafficking path, LAMP1 appears to be important in routing perforin to lytic granules. The lack of complete blocking of perforin transport to lysosomes is not surprising. It is not uncommon for lysosomal proteins to use different pathways to reach lysosomes. For example, a portion of lysosomal enzymes that normally use the MPR pathway is still sorted to lysosomes in cells

from I-cell disease patients (that do not have a functional MPR pathway).[40] Moreover, even though sorting of LAMP1 to lysosomes is mediated by adaptor complexes AP-1, AP-2, or AP-3, disrupting the function of any of these complexes does not completely block the delivery of LAMP1 to lysosomes.[32,41,42]

The interaction between LAMP1 and AP-1 complex is intriguing, as AP-1 is not required for the sorting of LAMP1.[43] AP-1 has been shown to interact with motor protein kinesin and function in delivery of cargo to lysosome-related melanosomes, and to facilitate movement of vesicles from the TGN.[44,45] That prompted us to ask whether LAMP1/AP-1 binding could play a role in the trafficking of perforin-containing transport vesicles to lytic granules. We found that disruption of expression of adaptin γ caused alteration of perforin trafficking and inhibited cytotoxicity, similar to effects observed in LAMP1 RNAi cells. Our data suggest that the direct interaction between LAMP1 and AP-1[32] could mediate transport of LAMP1-positive vesicles, containing perforin, to lytic granules. The lack of LAMP1 could prevent binding of AP-1 to perforin-positive vesicles and result in retention of perforin in the transport vesicles instead of its delivery to lytic granules. Similarly, the lack of AP-1 complex would prevent proper perforin transfer from the TGN to lytic granules because there would be no adaptor to interact with LAMP1 and enable the transport (Figure 7D).

Perforin is essential for the lytic activity of cytotoxic lymphocytes.[13,46] It is required for delivery and release of granzyme B to the cytoplasm of target cells.[47,48] Even a small decrease in perforin expression correlates with marked reduction in cytotoxicity.[49] NK cells do not release all of their lytic granules at once, only secreting a subset of the lytic granule pool following activation.[50] In addition, not all of the fusion events lead to full pore opening and release of granule content.[51] Furthermore, perforin is processed in lysosomes to give a mature form of the protein; an interesting possibility is that the impaired delivery of perforin to lysosomes could also affect the rate of its maturation. Thus, a decreased amount of perforin in lytic granules, or its improper maturation, could have a detrimental impact on NK-cell cytotoxicity. In this light, our data show that disruption of LAMP1 expression has a pleiotropic effect on NK cells, causing impairment of trafficking of a critical lytic granule protein, perforin, and slower movement of lytic granules. This results in the inability of NK cells to deliver granzyme B to target cells and inhibition of NK-cell cytotoxicity. Thus, LAMP1 is not only a marker of NK-cell degranulation, but also a crucial component of NK-cell cytotoxicity.

Acknowledgments

The authors thank Laurette Femnou and Claudine Jones for their support and technical help, Eric Long and Linjie Tian for their critical comments, and the NIH Clinical Center Department of Transfusion Medicine for providing the blood samples.

This work was supported by the intramural programs of the National Institute of Allergy and Infectious Diseases.

Authorship

Contribution: K.K., A.G.-K., V.N., and G.P. performed the experiments; K.K., A.G.-K., and V.N. analyzed the results; K.K. and A.G.-K. designed experiments; and K.K. and J.E.C. wrote the manuscript.

Conflict-of-interest disclosure: The authors declare no competing financial interests.

Correspondence: Konrad Krzewski, National Institute of Allergy and Infectious Diseases, National Institutes of Health, 12441 Parklawn Dr, Twinbrook II, Room 205, Rockville, MD 20852; e-mail: krzewskikj@niaid.nih.gov; and John E. Coligan, National Institute of Allergy and Infectious Diseases, National Institutes of Health, 12441 Parklawn Dr, Twinbrook II, Room 205, Rockville, MD 20852; e-mail: jcoligan@niaid.nih.gov.

References

1. Vivier E, Tomasello E, Baratin M, Walzer T, Ugolini S. Functions of natural killer cells. *Nat Immunol.* 2008;9(5):503-510.
2. Orange JS. Formation and function of the lytic NK-cell immunological synapse. *Nat Rev Immunol.* 2008;8(9):713-725.
3. Krzewski K, Coligan JE. Human NK cell lytic granules and regulation of their exocytosis. *Front Immunol.* 2012;3:335.
4. Voskoboinik I, Smyth MJ, Trapani JA. Perforin-mediated target-cell death and immune homeostasis. *Nat Rev Immunol.* 2006;6(12):940-952.
5. Pipkin ME, Lieberman J. Delivering the kiss of death: progress on understanding how perforin works. *Curr Opin Immunol.* 2007;19(3):301-308.
6. Talanian RV, Yang X, Turbov J, et al. Granule-mediated killing: pathways for granzyme B-initiated apoptosis. *J Exp Med.* 1997;186(8):1323-1331.
7. Beresford PJ, Xia Z, Greenberg AH, Lieberman J. Granzyme A loading induces rapid cytolysis and a novel form of DNA damage independently of caspase activation. *Immunity.* 1999;10(5):585-594.
8. Baetz K, Isaaz S, Griffiths GM. Loss of cytotoxic T lymphocyte function in Chediak-Higashi syndrome arises from a secretory defect that prevents lytic granule exocytosis. *J Immunol.* 1995;154(11):6122-6131.
9. Ménasché G, Pastural E, Feldmann J, et al. Mutations in RAB27A cause Griscelli syndrome associated with haemophagocytic syndrome. *Nat Genet.* 2000;25(2):173-176.
10. Clark RH, Stinchcombe JC, Day A, et al. Adaptor protein 3-dependent microtubule-mediated movement of lytic granules to the immunological synapse. *Nat Immunol.* 2003;4(11):1111-1120.
11. Feldmann J, Callebaut I, Raposo G, et al. Munc13-4 is essential for cytolytic granules fusion and is mutated in a form of familial hemophagocytic lymphohistiocytosis (FHL3). *Cell.* 2003;115(4):461-473.
12. Arneson LN, Brickshawana A, Segovis CM, Schoon RA, Dick CJ, Leibson PJ. Cutting edge: syntaxin 11 regulates lymphocyte-mediated secretion and cytotoxicity. *J Immunol.* 2007;179(6):3397-3401.
13. Bryceson YT, Rudd E, Zheng C, et al. Defective cytotoxic lymphocyte degranulation in syntaxin-11 deficient familial hemophagocytic lymphohistiocytosis 4 (FHL4) patients. *Blood.* 2007;110(6):1906-1915.
14. Marcet-Palacios M, Odemuyiwa SO, Coughlin JJ, et al. Vesicle-associated membrane protein 7 (VAMP-7) is essential for target cell killing in a natural killer cell line. *Biochem Biophys Res Commun.* 2008;366(3):617-623.
15. Wood SM, Meeths M, Chiang SC, et al. Different NK cell-activating receptors preferentially recruit Rab27a or Munc13-4 to perforin-containing granules for cytotoxicity. *Blood.* 2009;114(19):4117-4127.
16. Krzewski K, Gil-Krzewska A, Watts J, Stern JN, Strominger JL. VAMP4- and VAMP7-expressing vesicles are both required for cytotoxic granule exocytosis in NK cells. *Eur J Immunol.* 2011;41(11):3323-3329.
17. Burkhardt JK, Hester S, Lapham CK, Argon Y. The lytic granules of natural killer cells are dual-function organelles combining secretory and pre-lysosomal compartments. *J Cell Biol.* 1990;111(6, pt 1):2327-2340.
18. Peters PJ, Borst J, Oorschot V, et al. Cytotoxic T lymphocyte granules are secretory lysosomes, containing both perforin and granzymes. *J Exp Med.* 1991;173(5):1099-1109.
19. Saftig P, Klumperman J. Lysosome biogenesis and lysosomal membrane proteins: trafficking meets function. *Nat Rev Mol Cell Biol.* 2009;10(9):623-635.
20. Nishino I, Fu J, Tanji K, et al. Primary LAMP-2 deficiency causes X-linked vacuolar cardiomyopathy and myopathy (Danon disease). *Nature.* 2000;406(6798):906-910.
21. Tanaka Y, Guhde G, Suter A, et al. Accumulation of autophagic vacuoles and cardiomyopathy in

LAMP-2-deficient mice. *Nature.* 2000;406(6798): 902-906.

22. Andrejewski N, Punnonen EL, Guhde G, et al. Normal lysosomal morphology and function in LAMP-1-deficient mice. *J Biol Chem.* 1999; 274(18):12692-12701.
23. González-Polo RA, Boya P, Pauleau AL, et al. The apoptosis/autophagy paradox: autophagic vacuolization before apoptotic death. *J Cell Sci.* 2005;118(pt 14):3091-3102.
24. Huynh KK, Eskelinen EL, Scott CC, Malevanets A, Saftig P, Grinstein S. LAMP proteins are required for fusion of lysosomes with phagosomes. *EMBO J.* 2007;26(2):313-324.
25. Alter G, Malenfant JM, Altfeld M. CD107a as a functional marker for the identification of natural killer cell activity. *J Immunol Methods.* 2004;294 (1-2):15-22.
26. Packard BZ, Telford WG, Komoriya A, Henkart PA. Granzyme B activity in target cells detects attack by cytotoxic lymphocytes. *J Immunol.* 2007;179(6):3812-3820.
27. Thiery J, Walch M, Jensen DK, Martinvalet D, Lieberman J. Isolation of cytolytic T cell and NK granules and purification of their effector proteins. *Curr Prot Cell Biol.* 2010; Chapter 3:Unit 3.37.
28. Mentlik AN, Sanborn KB, Holzbaur EL, Orange JS. Rapid lytic granule convergence to the MTOC in natural killer cells is dependent on dynein but not cytolytic commitment. *Mol Biol Cell.* 2010; 21(13):2241-2256.
29. Hersperger AR, Makedonas G, Betts MR. Flow cytometric detection of perforin upregulation in human CD8 T cells. *Cytometry A.* 2008;73(11): 1050-1057.
30. Makedonas G, Banerjee PP, Pandey R, et al. Rapid up-regulation and granule-independent transport of perforin to the immunological synapse define a novel mechanism of antigen-specific CD8+ T cell cytotoxic activity. *J Immunol.* 2009; 182(9):5560-5569.
31. Hersperger AR, Pereyra F, Nason M, et al. Perforin expression directly ex vivo by HIV-specific CD8 T-cells is a correlate of HIV elite control. *PLoS Pathog.* 2010;6(5):e1000917.
32. Höning S, Griffith J, Geuze HJ, Hunziker W. The tyrosine-based lysosomal targeting signal in lamp-1 mediates sorting into Golgi-derived clathrin-coated vesicles. *EMBO J.* 1996;15(19): 5230-5239.
33. Andzelm MM, Chen X, Krzewski K, Orange JS, Strominger JL. Myosin IIA is required for cytolytic granule exocytosis in human NK cells. *J Exp Med.* 2007;204(10):2285-2291.
34. Johansson M, Rocha N, Zwart W, et al. Activation of endosomal dynein motors by stepwise assembly of Rab7-RILP-p150Glued, ORP1L, and the receptor betaIII spectrin. *J Cell Biol.* 2007; 176(4):459-471.
35. Daniele T, Hackmann Y, Ritter AT, et al. A role for Rab7 in the movement of secretory granules in cytotoxic T lymphocytes. *Traffic.* 2011;12(7): 902-911.
36. Reczek D, Schwake M, Schröder J, et al. LIMP-2 is a receptor for lysosomal mannose-6-phosphate-independent targeting of beta-glucocerebrosidase. *Cell.* 2007;131(4):770-783.
37. Burkhardt JK, Hester S, Argon Y. Two proteins targeted to the same lytic granule compartment undergo very different posttranslational processing. *Proc Natl Acad Sci USA.* 1989; 86(18):7128-7132.
38. van der Spoel A, Bonten E, d'Azzo A. Transport of human lysosomal neuraminidase to mature lysosomes requires protective protein/cathepsin A. *EMBO J.* 1998;17(6):1588-1597.
39. Brennan AJ, Chia J, Browne KA, et al. Protection from endogenous perforin: glycans and the C terminus regulate exocytic trafficking in cytotoxic lymphocytes. *Immunity.* 2011;34(6): 879-892.
40. Glickman JN, Kornfeld S. Mannose 6-phosphate-independent targeting of lysosomal enzymes in I-cell disease B lymphoblasts. *J Cell Biol.* 1993; 123(1):99-108.
41. Le Borgne R, Alconada A, Bauer U, Hoflack B. The mammalian AP-3 adaptor-like complex mediates the intracellular transport of lysosomal membrane glycoproteins. *J Biol Chem.* 1998; 273(45):29451-29461.
42. Janvier K, Bonifacino JS. Role of the endocytic machinery in the sorting of lysosome-associated membrane proteins. *Mol Biol Cell.* 2005;16(9): 4231-4242.
43. Meyer C, Zizioli D, Lausmann S, et al. mu1A-adaptin-deficient mice: lethality, loss of AP-1 binding and rerouting of mannose 6-phosphate receptors. *EMBO J.* 2000;19(10):2193-2203.
44. Delevoye C, Hurbain I, Tenza D, et al. AP-1 and KIF13A coordinate endosomal sorting and positioning during melanosome biogenesis. *J Cell Biol.* 2009;187(2):247-264.
45. Nakagawa T, Setou M, Seog D, et al. A novel motor, KIF13A, transports mannose-6-phosphate receptor to plasma membrane through direct interaction with AP-1 complex. *Cell.* 2000;103(4): 569-581.
46. Ishii E, Ueda I, Shirakawa R, et al. Genetic subtypes of familial hemophagocytic lymphohistiocytosis: correlations with clinical features and cytotoxic T lymphocyte/natural killer cell functions. *Blood.* 2005;105(9):3442-3448.
47. Keefe D, Shi L, Feske S, et al. Perforin triggers a plasma membrane-repair response that facilitates CTL induction of apoptosis. *Immunity.* 2005;23(3):249-262.
48. Thiery J, Keefe D, Boulant S, et al. Perforin pores in the endosomal membrane trigger the release of endocytosed granzyme B into the cytosol of target cells. *Nat Immunol.* 2011;12(8):770-777.
49. Portales P, Reynes J, Pinet V, et al. Interferon-alpha restores HIV-induced alteration of natural killer cell perforin expression in vivo. *AIDS.* 2003; 17(4):495-504.
50. Rak GD, Mace EM, Banerjee PP, Svitkina T, Orange JS. Natural killer cell lytic granule secretion occurs through a pervasive actin network at the immune synapse. *PLoS Biol.* 2011; 9(9):e1001151.
51. Liu D, Martina JA, Wu XS, Hammer JA III, Long EO. Two modes of lytic granule fusion during degranulation by natural killer cells. *Immunol Cell Biol.* 2011;89(6):728-738.